

MASTER OPTICAL POLARIZATION VARIABILITY DETECTION IN THE MICROQUASAR V404
CYG/GS2023+33

VLADIMIR M. LIPUNOV^{1,2}, E. GORBOVSKOY², V. KORNILOV^{1,2}, V. KRUSHINSKIY³, D. VLASENKO^{1,2}, N. TIURINA²,
P. BALANUTSA², A. KUZNETSOV², N. BUDNEV⁴, O. GRESS⁴, A. TLATOV⁵, R. REBOLO LOPEZ⁶, M. SERRA-RICART⁶, D. A. H.
BUCKLEY⁷, G. ISRAELYAN⁶, N. LODIEU⁶, K. IVANOV⁴, S. YAZEV⁴, YU. SERGIENKO⁸, A. GABOVICH⁸, V. YURKOV⁸, H. LEVATO⁹,
C. SAFFE⁹, R. PODESTA¹⁰, C. MALLAMACI¹⁰, C. LOPEZ¹⁰

M.V.Lomonosov Moscow State University, Physics Department, Leninskie gory, GSP-1, Moscow, 119991, Russia

M.V.Lomonosov Moscow State University, Sternberg Astronomical Institute, Universitetsky pr., 13, Moscow, 119234, Russia

Kourovka Astronomical Observatory, Ural Federal University, Lenin ave. 51, Ekaterinburg 620000, Russia

Applied Physics Institute, Irkutsk State University, 20, Gagarin blvd, 664003, Irkutsk, Russia

Kislovodsk Solar Station of the Main (Pulkovo) Observatory RAS, P.O.Box 45, ul. Gagarina 100, Kislovodsk 357700, Russia

Instituto de Astrofísica de Canarias, C/Vía Lctea, s/n E38205, La Laguna, Tenerife, Spain

South African Astronomical Observatory, P.O. Box 9, Observatory 7935, Cape Town, South Africa

Blagoveschensk State Pedagogical University, Lenin str., 104, Amur Region, Blagoveschensk 675000, Russia

Instituto de Ciencias Astronómicas, de la Tierra y del Espacio (ICATE), Av.España Sur 1512, J5402DSP, San Juan, Argentina

and

Observatorio Astronómico Félix Aguilar (OFA), Sede Central: Avda Benavides s/n, Rivadavia, El Leonsito, Argentina

ABSTRACT

On 2015 June 15 the Swift space observatory discovered that the Galactic black hole candidate V404 Cyg was undergoing another active X-ray phase, after 25 years of inactivity ([Barthelmy et al. 2015](#)). Twelve telescopes of the MASTER Global Robotic Net located at six sites across four continents were the first ground based observatories to start optical monitoring of the microquasar after its gamma-ray wakeup at 18h 34m 09s U.T. on 2015 June 15 ([Lipunov et al. 2015](#)). In this paper we report, for the first time, the discovery of variable optical linear polarization, changing by 4-6% over a timescale of ~ 1 h, on two different epochs. We can conclude that the additional variable polarization arises from the relativistic jet generated by the black hole in V404Cyg. The polarization variability correlates with optical brightness changes, increasing when the flux decreases.

Keywords: black holes, V404 Cyg — polarization — optical jet — x-ray nova — relativistic jet

1. INTRODUCTION

The X-ray nova GS 2023+338 was discovered on 1989 May 22 by the Ginga X-ray satellite (Makino et al. 1989). Soon after the object was identified with the variable star V404 Cyg, which had been seen to brighten by seven magnitudes in the optical in 1938 (Wagner et al. 1989a,b). It is now well established (Rodriguez et al. 2015) that V404 Cyg is a binary system consisting of a giant secondary star, older and less massive than the Sun and a primary star which is an accreting black hole candidate (Antokhina et al. 1993; Casares et al. 1991). The secondary (optical companion) is believed to undergo episodic enhanced mass loss every few decades, losing part of its mass to the black hole. This matter emits X-ray radiation while heating up to several hundred million degrees in the accretion disk. The detection of nonthermal radio and soft X-ray radiation (Rana et al. 2015), typically found in quasars, that are millions of times more massive and with powerful black holes residing in nuclei of active galaxies (i.e. AGN), led researchers to call this black hole a microquasar, ejecting relativistic particles in the form of jets. In this paper we report the detection, for the first time, of variable optical polarization arising in the relativistic jet generated by the black hole.

On 2015 June 15 the Swift space observatory found that one of the most securely identified Galactic stellar mass black hole candidates, the binary system V404 Cyg, began undergoing another active X-ray phase after 25 years of inactivity (Barthelmy et al. 2015).

The twin optical telescope, MASTER-Tunka of the MASTER Global Robotic Net (Lipunov et al. 2010), located near Lake Baikal (Lomonosov Moscow State University and Irkutsk State University Tunka astrophysical center), was the first ground-based observatory to point to V404 Cyg after the Swift alert. This was 22 sec after the notice time (Lipunov et al. 2015) of the burst alert, via space communication system (i.e. socket messages **GCN: The Gamma-ray Coordinates Network alert** (Barthelmy et al. 1994, 1995)) and after 150 seconds we detected a bright optical flare (Lipunov et al. 2015), reaching magnitude 14, with the star brightening by a factor of 2.5 in a mere half-hour. In the next few weeks six MASTER twin robotic telescopes performed about 20 pointings. Dozens of telescopes worldwide subsequently observed the object at various wavelengths (Rodriguez et al. (2015); Mooley et al. (2015); Munoz-Darias et al. (2015); Ferrigno et al. (2015); Motta et al. (2015); Tetarenko et al. (2015a,b); Tsubono et al. (2015)), but MASTER is the first to report on the discovery of variable optical linear polarization arising in the relativistic jet generated by the black hole.

2. MASTER GLOBAL ROBOTIC NETWORK OBSERVATION

The MASTER robotic telescopes¹ are a network of identical instruments deployed over several continents and equipped with identical CCD cameras capable of performing B,V,R,I (Johnson/Bessell) photometric and linear polarimetric observations (Lipunov et al. 2010; Kornilov et al. 2012; Pruzhinskaya et al. 2014). Each MASTER-II observatory has twin 0.40-m f/2.5 wide field reflectors (Hamilton design; see Kornilov et al. (2012)) and a prime focus 4k x 4k CCD camera, which provide a total 8 square-degree field and reaches to a white-light magnitude of 20-21 (in 180s exposure). In addition, the mounts for these two telescopes also have two very wide-field (VWF) optical cameras, with 800 square degrees field of view, reaching to magnitude of 15 (Lipunov et al. 2010; Kornilov et al. 2012). The observatories are located as follows: operating in Russia, from east to west, the MASTER-Amur, MASTER-Tunka, MASTER-Ural, and MASTER-Kislovodsk; the MASTER-SAAO in South Africa; the MASTER-IAC in the Canary Islands and MASTER-OAFA in Argentina.

The observations with MASTER-Net can be performed in three different modes: alert, survey and inspection. Alert mode is aimed at automated observations of rapid events, like Gamma Ray Bursts (GRBs) from SWIFT, Fermi, IPN, MAXI, INTEGRAL and gravitational wave or neutrino events. The primary goals of the MASTER Global Robotic Network are the rapid response to alerts (first, GRB alerts). The alert mode is triggered if a transient position has good accuracy (when the error-box size is less than $2^\circ \times 2^\circ$ MASTER FOV) and is typically used to observe GRBs upon receiving notices from the Gamma-ray Coordinates Network². In this alert mode MASTER observes with parallel 0.4-m telescopes, each covering the same field, and with polarizers (Lipunov et al. 2016), pointing just after the notice time. Exposure times follow the relation $t_{exp} = (T_{start} - T_0)/5$, where T_0 is the trigger time (UT), T_{start} is the time of the beginning of exposure (UT). The exposure time is rounded to an integer with a step of 10 s and does not exceed 3

¹ <http://observ.pereplet.ru>

² <http://gcn.gsfc.nasa.gov/>

min. All images are reduced automatically in real-time mode via our own software developed by the MASTER team over the past ten years. If we observe in survey or inspection mode, we usually observe in the white (unfiltered) light to increase the limiting magnitude. The corresponding internal photometric magnitudes can be described fairly well by the equation $W = 0.8 * R2 + 0.2 * B2$, where $R2$ and $B2$ are the second epoch DSS red and blue magnitudes, respectively, adopted from USNO-B1.0 catalog (Monet et al. 2003; Kornilov et al. 2012; Gorbovskoy et al. 2012).

The technique of polarimetric measurements used on MASTER network telescopes is considered in detail in (Pruzhinskaya et al. 2014). It allows detecting the *linear* polarization at 1-2% level for objects brighter than 14mag. We stress that MASTER-II consists of twin wide field telescopes each with a $2^\circ \times 2^\circ$ field. It gives us the possibility to determine the polarization for thousands stars from 12 to 16 magnitudes simultaneously. To estimate an error of the object's polarimetric measurement we select a few tens of field stars with similar brightness in the same frame and calculate the standard deviations of their polarizations, assuming that the stars have the same polarization produced by the ISM. Therefore, we calculate the error of polarization measurements as a chance fluctuations of the background stars, assuming that they have no variable polarization.

3. POLARIMETRY TECHNIQUE

The MASTER Net was designed with the objective to deliver polarization information as early as possible after GRB triggers. More than 100 observations of GRBs were made by the MASTER global robotic net. Optical emission was detected for ~ 20 GRBs (Lipunov et al. 2007; Gorbovskoy et al. 2012; Pruzhinskaya et al. 2014). The GRB 100906A, GRB 110422A, and GRB 121011A events deserved attention because their optical observations were carried out during the prompt gamma-ray emission.

The technique of polarimetric measurements used on MASTER network telescopes is considered in detail in (Pruzhinskaya et al. 2014) and although primarily designed for GRB followup, the same techniques can be used for polarimetry of other objects.

We only utilize linear polarizers for MASTER, so cannot determine the circular polarization of objects.

If we let I_1 and I_2 be the signals on the CCD detector with orthogonal polarizing filters (for example oriented with their axes at 45° and 135°), then a lower limit of the linear polarization is obtained from $P_{low} = (I_1 - I_2)/(I_1 + I_2)$.

To derive the degree of linear polarization, rather than a limit, one would need to perform observations with polarizers positioned at three angles, for example, at 0° , 45° , and 90° with respect to the reference direction. Since we have two fixed orthogonal filters at each of the MASTER-II telescopes, each telescope alone observes only a lower limit on polarization level — P_{low} .

If the value of P_{low} is less than measurement error σ_p , then formally we have zero as a minimum estimate for the degree of linear polarization. Even with a 100-percent linearly polarized source, it is still possible, if the polarizers were so positioned that linear polarization position was inclined exactly by 45° to both of them, to register zero polarization for the object.

The two synchronous frames (taken with different cameras) used to measure P_{low} are mutually calibrated so that the average P_{low} for comparison stars would be $Avg(P_{low}) = 0$. This is achieved at the stage of the photometric calibration. We use the same reference stars for frames in both polarizations from the USNO B-1 catalog (with no polarization measurements). This implies, for unpolarized sources, that $Avg(I_{45} - I_{135}) = 0$ and consequently $Avg(P_{low}) = 0$. If the reference stars are polarized (e.g. due to interstellar polarization, then they will show non-zero P_{low} . For the purpose of this paper, the exact measurement of the linear polarization value is not the aim, but rather the purpose is to establish the polarization variability of V404Cyg. Since the Galactic polarization is constant, it does not affect to the determination of polarization variability.

The MASTER polarization band is determined by the response curves of the CCD camera and a transmission curve of polarizing filter, which have been reviewed here (Pruzhinskaya et al. 2014).

For the determination of errors, we analyzed the distribution of P_{low} of the field reference stars, depending on the magnitude. Then we selected only the stars with magnitudes in the interval $m_{V404} \pm 0.5$, where m_{V404} is a V404 magnitude on a given frame. The dispersion of comparison stars P_{low} in this interval are used to define the $1 - \sigma$ error of object P_{low} . We use the reference stars in a radius of 0.5° for V404 Cyg. All errors that are reported in this paper are 1σ .

4. MASTER V404 CYG RESULTS

In the direction of V404 Cyg, strong interstellar polarization is observed due to scattering by Galactic dust, which is aligned with the Galactic magnetic field. Naturally this polarization is essentially constant, as noted in the very first reported observations of the new outburst of the microquasar (Blay et al. 2015; Itoh et al. 2015). The magnitude

and position angle measured for V404 Cyg in (Itoh et al. 2015) was found to be consistent with the interstellar linear polarization, at a level of about 8% and at a position angle of $\sim 15^\circ$, respectively.

The MASTER-Net observations were performed throughout 2015 June at the MASTER-Tunka and MASTER-Kislovodsk nodes. They reveal not only the constant interstellar polarization component during the earliest epochs of optical observations, but also polarization variations at certain epochs in a number of cases. The full description of the data reduction process, polarization standards, photometry and polarization measurements are described in (Pruzhinskaya et al. 2014).

We observed in two orthogonally related polarizers we detect the value $Y = (I_1 - I_2)/(I_1 + I_2)$. It's evident that Y is the low limit of linear polarization of the object. But the Y change (time evolution of Y) authentically proves the existence of an additional variable linear polarization, that is not connected with the interstellar dust.

As the Y value is measured in 2 polarizers with their fast axes orthogonal to each other, its variability is a result of the change of the E-vector, i.e. the degree of linear polarization and its position angle. The variability of flux in different polarizers can be explained by the variation of the contribution of polarized flux to the total flux. The degree of polarization increases when the unpolarized component of the optical flux of the system decreases relative to the contribution of the polarized flux. Therefore we expect the polarization to increase when the total optical brightness of system falls, say due to less X-ray irradiation of the secondary star. The polarized jet component then begins to dominate over the unpolarized reprocessed component, increasing the level of polarization.

We found at least two cases of bona fide linear polarization variability. The first event lasted a little more than an hour and was detected during alert observations on 2015 June 18. These observations were triggered by an INTEGRAL Alert (GCN, trigger Number 7029) following the detection of an X-ray burst. The MASTER-Tunka telescope automatically started observing the microquasar with the two parallel aligned telescope tubes, with mutually perpendicular polaroids, positioned along the North-South and East-West directions, 42 seconds after the trigger. At 15:36:00 UT MASTER-Tunka recorded the onset of an abrupt factor of six decrease of optical flux (Fig.1), followed by its recovery at an even higher level than the initial level. At the same time the polarization increased by $\sim 4\%$, reaching $\sim 12\%$, while it was of about $\sim 8\%$ before and after this event (one of the axes of our polarizer is aligned practically parallel to the position angle of the interstellar polarization (Tanaka et al. 2016)).

For the polarization measurements, we used the field stars with corresponding similar stellar magnitudes as the source, as follows. The error of the measurement is the standard deviation for the several measurements of the background stars. We use MASTER's wide fields (4 square degrees) to have measurements for thousands of field stars, many with magnitudes similar to V404 Cyg.

We observed the Y value to increase substantially, up to 12%, during V404 Cyg's fading. The error was estimated from reference stars where we found the chi-square statistical significance of this event to be 99.99%.

The second polarization variation event seen was recorded after receiving INTEGRAL alert N7035, on 2015 June. Twenty-seven seconds later, at 17:29:05UT, MASTER-Kislovodsk started photometric observations of V404 Cyg in two mutually perpendicular polarizations parallel and perpendicular to the meridian (i.e. 0° and 90°).

After two hours MASTER recorded strong and fast flux increases, accompanied by a decrease of polarization from 14% down to 8%. This result qualitatively corroborates the behavior found earlier in our MASTER-Tunka observations. The Tables of MASTER Y value and photometry data for V404 are available at <http://master.sai.msu.ru/static/V404tables.pdf>

5. INTERPRETATION AND DISCUSSION

The main source of the optical emission in V404 Cyg is the $0.7_{-0.2}^{+0.3} M_\odot$ K3 III-type subgiant companion (Casares et al. 1994; Shahbaz et al. 1994; Khargharia et al. 2010), including X-ray radiation reprocessed to optical on the illuminated side, facing the black hole. The intrinsic emission of the secondary (low-mass) star is practically undetectable during the time of the outburst, in which there is a factor of $\sim 10^8$, increase of the microquasar luminosity. Thus the rise of the optical flux during this outburst is primarily due to the heating of the low-mass star and, possibly, of the outer layers of the accretion disk. The accretion disk forms as a result of the mass loss from the giant star, through the L1 point of its Roche lobe, into the gravitational potential well of the black hole. While approaching the black hole the matter captured by it heats up to a temperature of several million degrees and emits the observed X-ray radiation.

However, there is yet another possible source of radiation in addition to the two mentioned above, namely a relativistic jet generated by the black hole and only observed until now in non-thermal radio and hard X-ray emission. We believe that this jet (or, more precisely, two symmetric bipolar jets) are responsible for the polarized optical emission.

Here is our proposed scenario for the observed 2015 June 18 polarization variation in the microquasar:

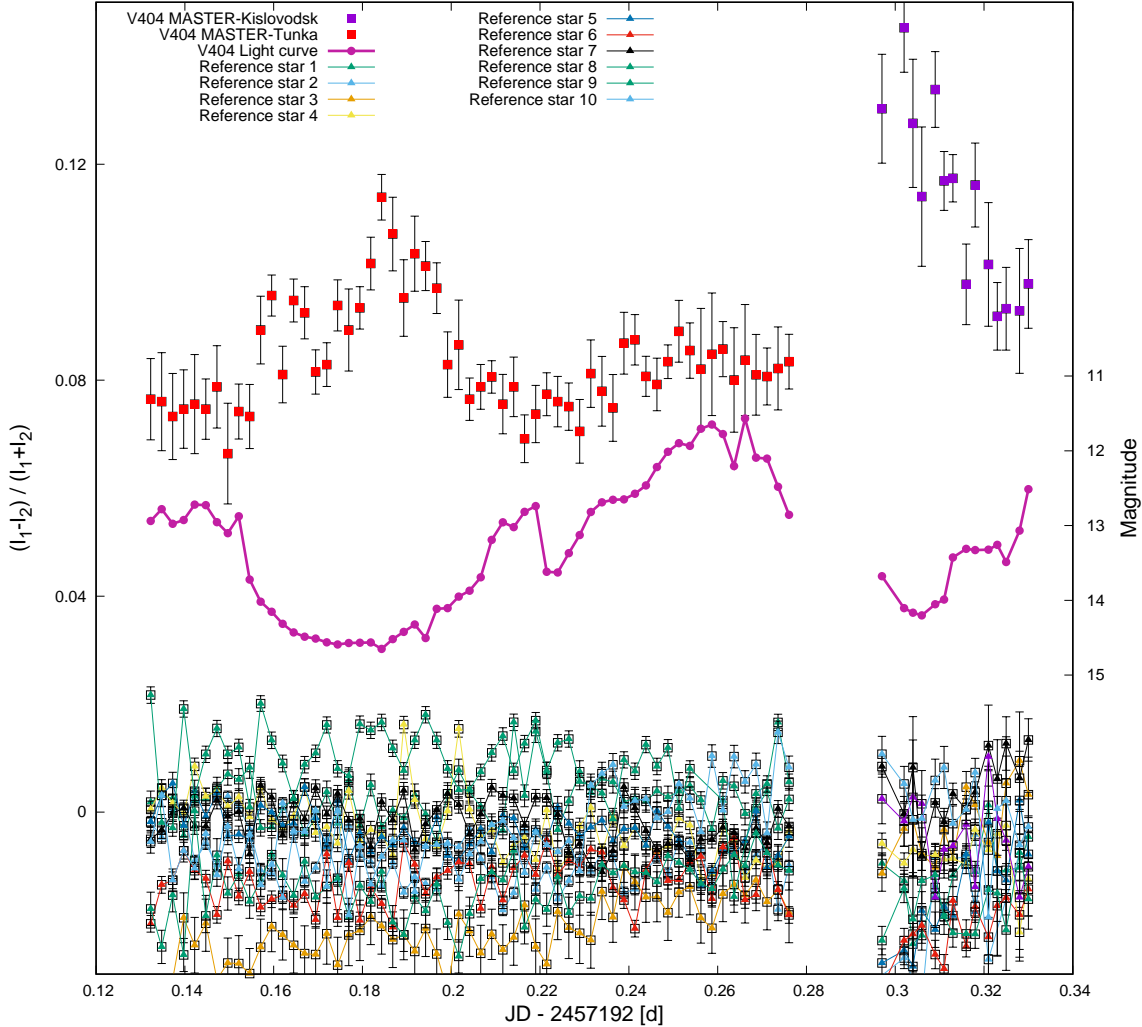


Figure 1. The variation of the $Y = (I_1 - I_2)/(I_1 + I_2)$ value of V404 Cyg microquasar based on MASTER-Tunka and MASTER-Kislovodsk observations. The data from MASTER-Tunka are up to 19:00 U.T, and from MASTER-Kislovodsk, after 19:00 U.T. There polarization of many field stars are also included. The behaviour of V404 light curve at the time of polarization variability is demonstrated by the magenta curve.

As the Y value is measured in two mutually perpendicular polarizers, its variability can be connected with variability of size of linear polarization or with turn of a vector of the polarization plane. The first explanation seems more preferably as it is difficult to imagine an essential variability of jet orientation on the times about tens of minutes. The variability of flux in different polarizers can be most possibly explained by the variability of the contribution of strongly polarized light in the general flux of an optical emission. Not incidentally, the polarization increases when the general optical flux of the system falls and the contribution polarization component grows. Anti-correlation between the value of polarization and brightness of an optical flux is apparently connected with the increase of jet contribution during the decreasing of the effect of warming up of an optical companion by x-ray emission arising near the black hole.

At 15:36:00 (UT) the accreting mass inflow began to decrease rapidly near the black hole, the region of maximum energy release. The X-ray flux also decreased and, as a result, so did the intensity of the heating of the secondary (giant) star. At the same time the active emission of the jet continued, because it is not directly associated with the instantaneous accretion rate but rather with the acceleration of relativistic particles near the black hole. In other

words, the jet became visible because its flux contribution increased with respect to the decrease of the luminosity of the irradiated secondary star. The jet emission is due to non-thermal synchrotron radiation and is therefore polarized, and hence its increased contribution resulted in the increase of the polarization of the total emission.

Strong linear polarization (up to $\sim 30\%$) is observed in the jets of BL Lac type objects, or blazars, namely quasars with relativistic jets pointing in the direction of the Earth. This is due to the synchrotron mechanism of their emission. Thus the discovery of non-thermal polarized optical component provides the direct evidence that the nature of one of the most secure black hole candidates, namely V404 Cyg, is similar to that of the millions of times more massive quasars (blazars). If we assume that the total jet polarization is equal to $\simeq 30\%$, as observed in blazar type objects, then the jets in V404 Cyg contribute about $K = L_j/L_o \sim 15\%$ to the total luminosity, implying a jet optical flux of about $2 \cdot 10^{-11} \text{ ergs}^{-1}\text{cm}^{-2}$. For the adopted distance of $2.39 \pm 0.14 \text{ kpc}$ (Miller et al. 2009) we obtain a total jet luminosity of $\sim 4 \cdot 10^{34} \text{ erg/s}$. The detection of unprecedentedly powerful non-thermal radio emission amounting to 6 Jy during outbursts (Tetarenko et al. 2015a) provides independent evidence confirming the likely existence of a non-thermal jet during this last outburst. This fact agrees quite well with jet flux estimates inferred in terms of the synchrotron emission mechanism.

During this paper's preparation, information about independent polarimetry observations was published (Tanaka et al. 2016), where the authors wrote that they didn't see polarization variability. We stress that we have a more extensive data set and also don't see polarization variability, except unequivocally at two different times, during rapid and deep optical flux decreases, which is the subject of the paper. The optical flux decrease was over a short timescale (compared to the scale of the several dozens days in total of the MASTER monitoring observations) and has the character of a rapid decrease of the optical flux of the system. The relative rarity of such events explains why were no other polarization variations have been seen in V404 Cyg (e.g. by Tanaka et al. (2016)).

ACKNOWLEDGMENTS

MASTER Global Robotic Net is supported in part by the Development Programm of Lomonosov Moscow State University. This work was also supported in part by RFBR 15-02-07875 grant, Russian Science Foundation 16-12-00085 and National Research Foundation of South Africa. We are grateful to Professor Tanaka for the information in his astro-ph paper, prior to publication. We are grateful to referee for the number of remarks and suggestions that have improved the paper.

REFERENCES

- Antokhina et al., 1993, AZh, 70, 804A
 Barthelmy S. et al. 2015, GCN, 17929, 1
 Barthelmy S. et al. 1994, AIP Conf. Proc., 307, 643
 Barthelmy S. et al. 1995, Ap&SS, 231, 235
 Blay et al. 2015, ATel, 7678, 1
 Casares J., Charles P. 1994, Nature, 355, 614
 Casares J., Charles P. A., Jones, D. H. P., et al. 1991, MNRAS, 250, 712
 Ferrigno et al. 2015, ATel 7662, 1
 Gorbovskoy E. et al., 2012, MNRAS, 421, 1874
 Gorbovskoy E. et al., 2016, MNRAS, 455, 3312
 Itoh et al. 2015, ATel 7709, 1
 Khargharia et al. 2010, Astrophys.J., 716, 1105
 Kimura M. et al. 2016, Nature, 529, 7584, pp. 54-58
 Kornilov et al., 2012, 2012, Experimental Astronomy, Vol. 33, Issue 1, pp.173-196, 2012
 Lipunov V. M. et al., 2007, Astronomy Reports, 51, 1004
 Lipunov V.M. et al. 2010, Advances in Astronomy, 349171
 Lipunov V.M.et al. 2015, ATel, 7696, 1
 Lipunov et al., 2015, MNRAS, 455, 712
 Makino F. et al. 1989, IAUC 4782, 1
 Miller-Jones et al., 2009, Mon. Not. R. Astron. Soc., 394, 1440
 Monet D. et al., 2003 Astron. J., Vol. 125, p. 984
 Mooley K. et al., 2015, ATel 7658, 1
 Motta et al. 2015, ATel 7666, 1
 Munoz-Darias et al. 2015, ATel 7659, 1
 Pruzhinskaya et al., 2014, New Astronomy, 29, 65
 Rana et al. 2015, Astrophys.J. in press, <http://arxiv.org/abs/1507.04049>
 Rodriguez et al. 2015, Astron. & Astrophys J.Let. in press, <http://arxiv.org/abs/1507.06659>
 Shahbaz et al. 1994, Mon. Not. R. Astron. Soc. 271, L10
 Tanaka et al. 2016, ApJ, 823, 35
 Tetarenko et al. 2015, ATel 7661, 1
 Tetarenko et al. 2015, ATel 7708, 1
 Tsubono et al. 2015, ATel 7701, 1
 Wagner R.M. et al. 1989a, IAUC 4783, 1
 Wagner R.M. et al. 1989b, IAUC 4797, 1

Table 1. Photometry of V404 Cyg by MASTER-Tunka Telescope in JD2457192.13-JD2457192.28 (EAST and WEST MASTER tubes)

JD	Filter	Tube	#1	#2	#3	#4	#5	#6	#7	#8	#9	#10	#11	#12	#13	#14	#15	#16	#17	#18	#19
2457192.1323	P	EAST	12.855	12.623	12.267	12.479	12.252	12.858	12.820	12.779	12.305	12.713	13.737	13.124	14.408	13.074	13.344	14.804	14.335	13.368	14.888
2457192.1348	P	EAST	12.698	12.679	12.260	12.476	12.245	12.848	12.819	12.760	12.307	12.742	13.798	13.147	14.334	13.073	13.326	14.842	14.327	13.380	14.834
2457192.1372	P	EAST	12.897	12.681	12.259	12.472	12.257	12.849	12.823	12.760	12.304	12.729	13.794	13.130	14.398	13.085	13.325	14.809	14.361	13.384	14.828
2457192.1397	P	EAST	12.845	12.687	12.263	12.473	12.266	12.856	12.831	12.752	12.303	12.716	13.757	13.158	14.401	13.076	13.315	14.810	14.367	13.373	14.775
2457192.1422	P	EAST	12.638	12.694	12.263	12.494	12.250	12.858	12.813	12.760	12.318	12.720	13.778	13.110	14.388	13.078	13.323	14.806	14.357	13.366	14.843
2457192.1447	P	EAST	12.646	12.689	12.257	12.488	12.253	12.860	12.822	12.759	12.313	12.720	13.764	13.132	14.398	13.071	13.310	14.812	14.346	13.385	14.859
2457192.1472	P	EAST	12.870	12.683	12.265	12.492	12.253	12.851	12.813	12.771	12.307	12.713	13.766	13.126	14.374	13.079	13.330	14.766	14.348	13.367	14.796
2457192.1496	P	EAST	13.030	12.695	12.260	12.480	12.258	12.868	12.818	12.758	12.316	12.722	13.769	13.134	14.383	13.077	13.329	14.777	14.347	13.372	14.804
2457192.1521	P	EAST	12.795	12.697	12.250	12.475	12.258	12.873	12.827	12.760	12.315	12.717	13.778	13.138	14.386	13.091	13.326	14.796	14.343	13.374	14.775
2457192.1546	P	EAST	13.644	12.680	12.252	12.477	12.258	12.851	12.824	12.762	12.305	12.739	13.781	13.137	14.364	13.077	13.324	14.817	14.314	13.368	14.813
2457192.1571	P	EAST	13.922	12.679	12.268	12.479	12.242	12.869	12.824	12.768	12.309	12.722	13.751	13.131	14.384	13.089	13.315	14.810	14.341	13.365	14.784
2457192.1595	P	EAST	14.050	12.695	12.267	12.488	12.259	12.862	12.824	12.772	12.314	12.706	13.766	13.115	14.365	13.079	13.315	14.814	14.346	13.362	14.809
2457192.1620	P	EAST	14.227	12.690	12.264	12.460	12.255	12.868	12.831	12.767	12.319	12.734	13.788	13.124	14.382	13.090	13.313	14.829	14.316	13.371	14.793
2457192.1645	P	EAST	14.326	12.704	12.264	12.482	12.260	12.859	12.819	12.767	12.322	12.722	13.792	13.126	14.403	13.072	13.311	14.807	14.335	13.364	14.815
2457192.1670	P	EAST	14.386	12.507	12.270	12.493	12.257	12.860	12.804	12.765	12.311	12.719	13.790	13.132	14.385	13.066	13.311	14.800	14.336	13.359	14.825
2457192.1695	P	EAST	14.423	12.711	12.265	12.490	12.263	12.875	12.807	12.765	12.324	12.713	13.772	13.129	14.386	13.061	13.312	14.808	14.319	13.363	14.815
2457192.1719	P	EAST	14.473	12.695	12.254	12.477	12.256	12.881	12.824	12.754	12.315	12.723	13.772	13.134	14.396	13.085	13.300	14.808	14.332	13.375	14.816
2457192.1744	P	EAST	14.489	12.702	12.262	12.497	12.267	12.860	12.805	12.768	12.311	12.717	13.776	13.121	14.384	13.062	13.320	14.821	14.326	13.354	14.782
2457192.1769	P	EAST	14.474	12.708	12.252	12.467	12.245	12.881	12.837	12.748	12.317	12.733	13.796	13.151	14.388	13.092	13.306	14.844	14.304	13.377	14.783
2457192.1794	P	EAST	14.467	12.699	12.262	12.487	12.267	12.864	12.817	12.761	12.327	12.720	13.763	13.128	14.393	13.072	13.304	14.839	14.316	13.365	14.806
2457192.1818	P	EAST	14.453	12.709	12.249	12.477	12.261	12.866	12.823	12.754	12.328	12.730	13.779	13.140	14.396	13.087	13.298	14.812	14.322	13.372	14.802
2457192.1843	P	EAST	14.526	12.706	12.261	12.491	12.271	12.845	12.819	12.761	12.331	12.717	13.769	13.127	14.377	13.073	13.309	14.823	14.334	13.369	14.795
2457192.1868	P	EAST	14.402	12.711	12.259	12.486	12.268	12.851	12.814	12.764	12.332	12.724	13.779	13.145	14.366	13.072	13.317	14.808	14.313	13.357	14.796
2457192.1893	P	EAST	14.318	12.694	12.265	12.493	12.268	12.861	12.818	12.748	12.318	12.714	13.791	13.148	14.374	13.068	13.316	14.848	14.333	13.355	14.803
2457192.1918	P	EAST	14.212	12.709	12.257	12.482	12.252	12.872	12.820	12.744	12.332	12.732	13.773	13.144	14.382	13.081	13.313	14.829	14.284	13.368	14.804
2457192.1942	P	EAST	14.395	12.712	12.265	12.485	12.272	12.852	12.828	12.751	12.335	12.720	13.771	13.141	14.372	13.069	13.307	14.790	14.316	13.361	14.834
2457192.1967	P	EAST	14.009	12.702	12.270	12.491	12.273	12.857	12.815	12.748	12.327	12.718	13.779	13.134	14.375	13.068	13.322	14.815	14.315	13.358	14.808
2457192.1992	P	EAST	14.015	12.701	12.259	12.478	12.261	12.872	12.828	12.748	12.314	12.723	13.783	13.150	14.365	13.077	13.319	14.839	14.306	13.359	14.781
2457192.2017	P	EAST	13.857	12.715	12.252	12.478	12.258	12.872	12.832	12.740	12.324	12.723	13.790	13.155	14.378	13.088	13.305	14.812	14.319	13.371	14.804
2457192.2041	P	EAST	13.788	12.718	12.257	12.468	12.268	12.866	12.827	12.748	12.321	12.729	13.798	13.150	14.380	13.074	13.315	14.818	14.326	13.367	14.812
2457192.2066	P	EAST	13.607	12.728	12.260	12.484	12.269	12.865	12.819	12.747	12.337	12.726	13.784	13.135	14.386	13.073	13.308	14.815	14.311	13.369	14.839
2457192.2091	P	EAST	13.104	12.728	12.275	12.488	12.269	12.863	12.820	12.747	12.338	12.719	13.786	13.140	14.388	13.068	13.303	14.804	14.344	13.348	14.797
2457192.2116	P	EAST	12.874	12.707	12.271	12.498	12.274	12.860	12.815	12.748	12.324	12.715	13.780	13.130	14.385	13.061	13.306	14.807	14.318	13.348	14.789
2457192.2141	P	EAST	12.935	12.718	12.265	12.491	12.274	12.863	12.808	12.750	12.333	12.721	13.788	13.129	14.396	13.068	13.312	14.830	14.354	13.354	14.800
2457192.2165	P	EAST	12.742	12.710	12.261	12.472	12.264	12.878	12.834	12.731	12.320	12.730	13.782	13.157	14.381	13.084	13.294	14.815	14.342	13.370	14.802
2457192.2190	P	EAST	12.660	12.715	12.276	12.490	12.270	12.869	12.813	12.748	12.337	12.714	13.779	13.129	14.408	13.066	13.294	14.841	14.354	13.343	14.821
2457192.2215	P	EAST	13.534	12.709	12.262	12.483	12.262	12.878	12.828	12.741	12.322	12.724	13.786	13.144	14.379	13.073	13.312	14.850	14.349	13.357	14.781
2457192.2240	P	EAST	13.546	12.713	12.273	12.487	12.277	12.864	12.811	12.746	12.339	12.715	13.778	13.132	14.421	13.063	13.301	14.833	14.333	13.349	14.822
2457192.2265	P	EAST	13.288	12.728	12.265	12.481	12.265	12.873	12.816	12.744	12.331	12.727	13.791	13.142	14.391	13.072	13.304	14.861	14.334	13.356	14.793
2457192.2289	P	EAST	13.051	12.724	12.255	12.479	12.254	12.891	12.819	12.739	12.324	12.736	13.800	13.136	14.404	13.087	13.298	14.839	14.315	13.363	14.797
2457192.2314	P	EAST	12.916	12.720	12.259	12.475	12.273	12.886	12.822	12.738	12.315	12.727	13.797	13.145	14.387	13.068	13.306	14.863	14.341	13.359	14.805
2457192.2339	P	EAST	12.889	12.722	12.255	12.479	12.264	12.889	12.821	12.742	12.322	12.727	13.809	13.139	14.400	13.070	13.308	14.838	14.322	13.364	14.814
2457192.2364	P	EAST	12.866	12.716	12.269	12.488	12.271	12.882	12.815	12.748	12.326	12.707	13.788	13.132	14.418	13.069	13.297	14.868	14.342	13.345	14.821
2457192.2389	P	EAST	12.796	12.731	12.270	12.487	12.269	12.873	12.806	12.752	12.339	12.716	13.802	13.135	14.410	13.069	13.295	14.836	14.341	13.352	14.815

JD	Filter	Tube	#1	#2	#3	#4	#5	#6	#7	#8	#9	#10	#11	#12	#13	#14	#15	#16	#17	#18	#19
2457192.2414	P	EAST	12.690	12.733	12.266	12.475	12.269	12.885	12.817	12.740	12.341	12.727	13.790	13.138	14.414	13.073	13.293	14.847	14.334	13.354	14.809
2457192.2438	P	EAST	12.451	12.722	12.265	12.471	12.273	12.890	12.820	12.737	12.324	12.728	13.799	13.137	14.407	13.072	13.298	14.844	14.355	13.358	14.790
2457192.2463	P	EAST	12.244	12.730	12.265	12.482	12.260	12.871	12.817	12.747	12.341	12.728	13.792	13.133	14.416	13.075	13.288	14.842	14.351	13.359	14.831
2457192.2488	P	EAST	12.127	12.723	12.261	12.475	12.257	12.887	12.820	12.748	12.335	12.734	13.799	13.135	14.424	13.072	13.294	14.871	14.339	13.355	14.781
2457192.2513	P	EAST	12.166	12.733	12.265	12.469	12.265	12.882	12.828	12.738	12.329	12.731	13.789	13.150	14.415	13.075	13.288	14.858	14.351	13.358	14.825
2457192.2538	P	EAST	11.936	12.732	12.264	12.468	12.275	12.879	12.828	12.734	12.328	12.727	13.637	13.138	14.419	13.076	13.298	14.837	14.346	13.364	14.818
2457192.2562	P	EAST	11.875	12.720	12.273	12.479	12.275	12.870	12.816	12.741	12.341	12.722	13.669	13.134	14.433	13.070	13.296	14.851	14.352	13.355	14.826
2457192.2587	P	EAST	12.007	12.732	12.265	12.478	12.263	12.881	12.824	12.740	12.333	12.730	13.752	13.135	14.420	13.076	13.279	14.835	14.355	13.354	14.825
2457192.2612	P	EAST	12.435	12.731	12.270	12.476	12.276	12.874	12.823	12.731	12.331	12.731	13.796	13.142	14.421	13.066	13.290	14.849	14.354	13.356	14.852
2457192.2637	P	EAST	11.793	12.727	12.272	12.481	12.272	12.876	12.806	12.749	12.326	12.723	13.687	13.131	14.415	13.064	13.301	14.859	14.364	13.351	14.785
2457192.2662	P	EAST	12.323	12.738	12.273	12.482	12.277	12.866	12.812	12.747	12.342	12.722	13.711	13.134	14.428	13.059	13.296	14.857	14.367	13.350	14.815
2457192.2687	P	EAST	12.332	12.733	12.269	12.474	12.267	12.882	12.824	12.738	12.329	12.724	13.798	13.140	14.427	13.073	13.291	14.854	14.343	13.357	14.826
2457192.2711	P	EAST	12.704	12.733	12.279	12.485	12.274	12.874	12.815	12.745	12.342	12.715	13.787	13.134	14.420	13.062	13.286	14.864	14.367	13.350	14.805
2457192.2736	P	EAST	13.082	12.728	12.273	12.476	12.265	12.880	12.812	12.749	12.330	12.728	13.794	13.138	14.416	13.071	13.288	14.870	14.343	13.352	14.795
2457192.2761	P	EAST	13.021	12.726	12.273	12.473	12.282	12.872	12.816	12.740	12.328	12.726	13.803	13.135	14.409	13.061	13.294	14.895	14.365	13.352	14.806
2457192.2786	P	EAST	12.655	12.744	12.274	12.483	12.273	12.879	12.812	12.751	12.334	12.721	13.781	13.131	14.411	13.061	13.298	14.840	14.352	13.337	14.791

JD	Filter	Tube	#1	#2	#3	#4	#5	#6	#7	#8	#9	#10	#11	#12	#13	#14	#15	#16	#17	#18	#19
2457192.1323	P	WEST	13.021	12.752	12.238	12.442	12.220	12.871	12.783	12.701	12.280	12.669	13.751	13.052	14.544	13.029	13.225	14.955	14.404	13.319	14.771
2457192.1348	P	WEST	12.863	12.750	12.226	12.425	12.214	12.866	12.785	12.690	12.273	12.694	13.753	13.052	14.582	13.039	13.200	15.012	14.388	13.284	14.778
2457192.1372	P	WEST	13.056	12.748	12.224	12.432	12.220	12.863	12.794	12.692	12.282	12.688	13.747	13.056	14.547	13.017	13.217	15.066	14.407	13.281	14.765
2457192.1397	P	WEST	13.007	12.740	12.219	12.440	12.231	12.854	12.791	12.702	12.279	12.683	13.764	13.066	14.571	13.026	13.238	14.953	14.402	13.300	14.738
2457192.1422	P	WEST	12.802	12.759	12.228	12.435	12.229	12.854	12.782	12.697	12.290	12.675	13.745	13.071	14.565	13.016	13.230	15.000	14.369	13.291	14.774
2457192.1447	P	WEST	12.808	12.744	12.226	12.439	12.223	12.865	12.784	12.696	12.287	12.678	13.751	13.054	14.552	13.026	13.229	15.000	14.376	13.305	14.745
2457192.1472	P	WEST	13.041	12.745	12.239	12.435	12.226	12.859	12.785	12.694	12.289	12.682	13.764	13.073	14.561	13.018	13.227	14.999	14.377	13.299	14.730
2457192.1497	P	WEST	13.174	12.740	12.236	12.447	12.221	12.872	12.769	12.699	12.281	12.681	13.753	13.062	14.540	13.032	13.229	14.993	14.348	13.299	14.727
2457192.1521	P	WEST	12.956	12.744	12.226	12.440	12.227	12.859	12.781	12.689	12.285	12.680	13.767	13.076	14.545	13.031	13.228	14.997	14.387	13.289	14.749
2457192.1546	P	WEST	13.803	12.744	12.233	12.433	12.219	12.865	12.776	12.701	12.287	12.685	13.746	13.064	14.578	13.031	13.222	14.992	14.377	13.292	14.756
2457192.1571	P	WEST	14.116	12.748	12.226	12.420	12.216	12.866	12.791	12.694	12.289	12.697	13.759	13.068	14.564	13.024	13.225	14.977	14.385	13.293	14.735
2457192.1595	P	WEST	14.258	12.747	12.227	12.429	12.222	12.854	12.790	12.703	12.288	12.678	13.761	13.064	14.562	13.024	13.235	14.996	14.405	13.296	14.726
2457192.1620	P	WEST	14.403	12.739	12.230	12.428	12.213	12.857	12.790	12.698	12.295	12.689	13.772	13.063	14.558	13.020	13.228	14.995	14.395	13.295	14.748
2457192.1645	P	WEST	14.532	12.738	12.234	12.438	12.223	12.861	12.779	12.694	12.287	12.692	13.762	13.057	14.554	13.029	13.222	15.001	14.393	13.288	14.772
2457192.1670	P	WEST	14.587	12.731	12.229	12.433	12.235	12.860	12.782	12.700	12.291	12.684	13.777	13.080	14.542	13.026	13.222	14.996	14.390	13.295	14.744
2457192.1695	P	WEST	14.600	12.748	12.230	12.435	12.222	12.864	12.772	12.689	12.292	12.690	13.763	13.062	14.568	13.029	13.222	14.992	14.401	13.294	14.741
2457192.1719	P	WEST	14.653	12.745	12.227	12.431	12.215	12.863	12.775	12.702	12.296	12.687	13.772	13.069	14.544	13.020	13.216	14.995	14.394	13.297	14.739
2457192.1744	P	WEST	14.693	12.746	12.223	12.435	12.220	12.863	12.775	12.691	12.290	12.690	13.759	13.060	14.552	13.028	13.224	15.002	14.400	13.291	14.756
2457192.1769	P	WEST	14.668	12.734	12.230	12.427	12.219	12.859	12.783	12.693	12.300	12.695	13.776	13.074	14.571	13.016	13.222	15.016	14.403	13.293	14.753
2457192.1794	P	WEST	14.670	12.738	12.226	12.439	12.225	12.863	12.778	12.687	12.293	12.687	13.768	13.068	14.575	13.028	13.226	15.011	14.401	13.287	14.749
2457192.1819	P	WEST	14.674	12.755	12.228	12.425	12.222	12.863	12.775	12.692	12.286	12.684	13.780	13.072	14.571	13.026	13.224	14.995	14.412	13.287	14.758
2457192.1843	P	WEST	14.774	12.748	12.223	12.429	12.230	12.854	12.777	12.692	12.295	12.689	13.773	13.071	14.576	13.023	13.231	14.987	14.400	13.283	14.762
2457192.1868	P	WEST	14.635	12.749	12.227	12.433	12.218	12.861	12.768	12.685	12.291	12.688	13.772	13.068	14.577	13.028	13.233	14.997	14.419	13.291	14.748
2457192.1893	P	WEST	14.525	12.748	12.227	12.425	indef	12.855	12.776	12.700	12.298	12.687	13.772	13.063	14.575	13.021	13.231	15.041	14.406	13.290	14.765
2457192.1918	P	WEST	14.437	12.751	12.233	12.425	12.226	12.857	12.777	12.692	12.298	12.686	13.771	13.079	14.569	13.018	13.226	15.002	14.393	13.294	14.764
2457192.1942	P	WEST	14.615	12.741	12.234	12.426	12.231	12.853	12.784	12.688	12.304	12.685	13.780	13.071	14.576	13.025	13.230	15.032	14.408	13.296	14.754
2457192.1967	P	WEST	14.220	12.749	12.226	12.428	12.227	12.860	12.781	12.690	12.295	12.687	13.776	13.073	14.569	13.023	13.233	15.013	14.403	13.288	14.744
2457192.1992	P	WEST	14.195	12.750	12.230	12.429	12.225	12.857	12.774	12.688	12.297	12.694	13.764	13.069	14.575	13.028	13.210	15.013	14.399	13.292	14.750
2457192.2017	P	WEST	14.045	12.744	12.235	12.430	indef	12.866	12.779	12.686	12.290	12.692	13.765	13.063	14.576	13.027	13.230	15.020	14.408	13.287	14.741
2457192.2041	P	WEST	13.954	12.755	12.230	12.426	12.234	12.855	12.779	12.692	12.301	12.685	13.772	13.074	14.558	13.022	13.232	15.003	14.404	13.284	14.747
2457192.2066	P	WEST	13.778	12.743	12.230	12.433	12.227	12.860	12.780	12.676	12.301	12.693	13.768	13.076	14.575	13.029	13.219	15.017	14.404	13.288	14.728
2457192.2091	P	WEST	13.279	12.748	12.234	12.426	12.226	12.853	12.768	12.689	12.301	12.693	13.774	13.080	14.582	13.027	13.218	15.024	14.404	13.290	14.754
2457192.2116	P	WEST	13.038	12.739	12.233	12.428	12.223	12.860	12.783	12.682	12.302	12.691	13.780	13.072	14.576	13.027	13.220	15.031	14.410	13.286	14.768
2457192.2141	P	WEST	13.106	12.750	indef	12.422	12.224	12.858	12.769	12.691	12.302	12.690	13.768	13.077	14.590	13.021	13.225	15.024	14.411	13.296	14.757
2457192.2165	P	WEST	12.892	12.745	12.231	12.428	12.217	12.861	12.783	12.677	12.305	12.688	13.773	13.074	14.586	13.023	13.220	15.019	14.415	13.288	14.770
2457192.2190	P	WEST	12.820	12.753	indef	12.426	12.218	12.862	12.773	12.690	12.298	12.687	13.783	13.061	14.598	13.025	13.207	15.043	14.433	13.289	14.743
2457192.2215	P	WEST	13.702	12.740	12.240	12.423	12.225	12.865	12.779	12.692	12.295	12.692	13.765	13.067	14.589	13.022	13.213	15.023	14.406	13.298	14.760
2457192.2240	P	WEST	13.711	12.745	12.236	12.422	12.224	12.864	12.783	12.691	12.302	12.684	13.776	13.076	14.585	13.017	13.231	15.032	14.417	13.298	14.758
2457192.2265	P	WEST	13.451	12.758	12.235	12.419	12.213	12.869	12.777	12.690	12.299	12.676	13.786	13.067	14.591	13.026	13.223	15.048	14.420	13.291	14.768
2457192.2289	P	WEST	13.204	12.746	12.238	12.427	12.215	12.870	12.776	12.684	12.296	12.690	13.779	13.069	14.577	13.030	13.216	15.034	14.416	13.278	14.732
2457192.2314	P	WEST	13.072	12.748	indef	12.426	12.220	12.877	12.783	12.684	12.303	12.676	13.772	13.075	14.584	13.028	13.217	15.038	14.420	13.289	14.745
2457192.2339	P	WEST	13.030	12.739	12.245	12.427	12.219	12.872	12.778	12.683	12.299	12.695	13.762	13.065	14.583	13.022	13.215	15.029	14.425	13.288	14.748
2457192.2364	P	WEST	13.048	12.748	12.245	12.422	12.222	12.861	12.779	12.680	12.300	12.695	13.775	13.072	14.591	13.023	13.213	15.023	14.420	13.290	14.753
2457192.2389	P	WEST	12.972	12.745	12.249	12.423	12.216	12.870	12.774	12.682	12.303	12.692	13.785	13.070	14.592	13.018	13.212	15.037	14.420	13.296	14.750
2457192.2414	P	WEST	12.841	12.738	12.245	12.425	12.211	12.877	12.778	12.680	12.293	12.697	13.773	13.062	14.604	13.026	13.215	15.043	14.412	13.282	14.756

JD	Filter	Tube	#1	#2	#3	#4	#5	#6	#7	#8	#9	#10	#11	#12	#13	#14	#15	#16	#17	#18	#19
2457192.2438	P	WEST	12.600	12.745	12.235	12.425	12.213	12.870	12.777	12.680	12.303	12.687	13.781	13.073	14.597	13.024	13.216	15.045	14.438	13.289	14.751
2457192.2463	P	WEST	12.409	12.742	12.243	12.422	12.216	12.858	12.787	12.681	12.308	12.693	13.782	13.074	14.581	13.025	13.223	15.038	14.420	13.290	14.755
2457192.2488	P	WEST	12.301	12.745	12.235	12.427	12.221	12.863	12.774	12.677	12.303	12.690	13.774	13.075	14.611	13.023	13.219	15.045	14.414	13.289	14.752
2457192.2513	P	WEST	12.334	12.754	12.243	12.423	12.222	12.864	12.778	12.674	12.292	12.688	13.783	13.070	14.613	13.030	13.214	15.030	14.424	13.294	14.762
2457192.2538	P	WEST	12.102	12.747	12.235	12.423	12.217	12.857	12.770	12.680	12.297	12.694	13.783	13.071	14.599	13.032	13.212	15.037	14.423	13.289	14.772
2457192.2562	P	WEST	indef	12.741	12.243	12.429	12.210	12.857	12.772	12.684	12.303	12.699	13.776	13.066	14.586	13.025	13.217	15.036	14.426	13.284	14.750
2457192.2587	P	WEST	12.172	12.747	12.242	12.423	12.217	12.849	12.783	12.675	12.311	12.694	13.776	13.082	14.588	13.014	13.215	15.061	14.417	13.286	14.773
2457192.2612	P	WEST	12.581	12.740	12.241	12.427	12.209	12.862	12.777	12.681	12.296	12.699	13.780	13.061	14.597	13.024	13.212	15.032	14.436	13.288	14.769
2457192.2637	P	WEST	11.965	12.754	12.244	12.424	12.222	12.858	12.777	12.675	12.301	12.693	13.772	13.069	14.602	13.018	13.222	15.041	14.432	13.287	14.751
2457192.2662	P	WEST	12.482	12.737	12.233	12.430	12.221	12.855	12.772	12.684	12.303	12.691	13.781	13.070	14.605	13.028	13.218	15.027	14.423	13.294	14.763
2457192.2687	P	WEST	12.496	12.748	12.244	12.419	12.222	12.858	12.785	12.675	12.307	12.691	13.778	13.078	14.594	13.024	13.220	15.047	14.426	13.285	14.760
2457192.2711	P	WEST	12.865	12.738	12.246	12.422	12.217	12.874	12.780	12.686	12.298	12.693	13.793	13.071	14.597	13.015	13.211	15.050	14.440	13.285	14.739
2457192.2736	P	WEST	13.256	12.746	12.241	12.423	12.225	12.860	12.769	12.680	12.304	12.694	13.779	13.085	14.612	13.017	13.210	15.028	14.425	13.290	14.755
2457192.2761	P	WEST	13.179	12.747	12.238	12.421	12.225	12.867	12.781	12.683	12.307	12.693	13.786	13.073	14.579	13.021	13.213	15.042	14.431	13.283	14.770
2457192.2786	P	WEST	12.808	12.744	12.243	12.415	12.218	12.869	12.775	12.697	12.294	12.696	13.778	13.072	14.575	13.019	13.207	15.042	14.453	13.290	14.751

JD	#1	#2	#3	#4	#5	#6	#7	#8	#9	#10	#11	#12	#13	#14	#15	#16	#17	#18	#19
2457192.2687	0.07556	0.00709	-0.01133	-0.02514	-0.02054	-0.01087	-0.01777	-0.02882	-0.00995	-0.01501	-0.00903	-0.02836	0.07694	-0.02238	-0.03250	0.08883	0.03839	-0.03296	-0.03020
2457192.2711	0.07419	0.00249	-0.01501	-0.02882	-0.02606	0.00018	-0.01593	-0.02698	-0.02008	-0.00995	0.00295	-0.02882	0.08151	-0.02146	-0.03434	0.08563	0.03379	-0.02974	-0.03020
2457192.2736	0.08014	0.00847	-0.01455	-0.02422	-0.01823	-0.00903	-0.01962	-0.03158	-0.01179	-0.01547	-0.00672	-0.02422	0.09020	-0.02468	-0.03572	0.07282	0.03793	-0.02836	-0.01823
2457192.2761	0.07282	0.00985	-0.01593	-0.02376	-0.02606	-0.00212	-0.01593	-0.02606	-0.00949	-0.01501	-0.00764	-0.02836	0.07831	-0.01823	-0.03710	0.06778	0.03057	-0.03158	-0.01639
2457192.2786	0.07053	0.00018	-0.01409	-0.03112	-0.02514	-0.00442	-0.01685	-0.02468	-0.01823	-0.01133	-0.00120	-0.02698	0.07556	-0.01916	-0.04170	0.09294	0.04666	-0.02146	-0.01823

JD	Filter	Tube	#1	#2	#3	#4	#5	#6	#7	#8	#9	#10	#11	#12	#13	#14	#15	#16	#17	#18	#19
2457192.3020	P	EAST	13.940	12.662	12.260	12.463	12.235	12.866	12.803	12.724	12.306	12.696	13.788	13.110	14.422	13.038	13.260	14.831	14.316	13.326	14.793
2457192.3040	P	EAST	14.014	12.638	12.262	12.462	12.239	12.863	12.810	12.718	12.308	12.698	13.784	13.108	14.440	13.036	13.248	14.860	14.316	13.328	14.787
2457192.3060	P	EAST	14.064	12.626	12.248	12.460	12.238	12.854	12.800	12.731	12.297	12.701	13.787	13.114	14.459	13.041	13.254	14.850	14.313	13.335	14.810
2457192.3090	P	EAST	13.918	12.613	12.254	12.466	12.241	12.868	12.795	12.724	12.303	12.694	13.793	13.108	14.435	13.032	13.250	14.847	14.329	13.329	14.829
2457192.3110	P	EAST	13.863	12.477	12.258	12.455	12.239	12.859	12.800	12.730	12.300	12.703	13.803	13.109	14.447	13.041	13.254	14.862	14.329	13.331	14.806
2457192.3130	P	EAST	13.302	12.538	12.260	12.466	12.244	12.853	12.789	12.730	12.292	12.701	13.794	13.118	14.452	13.046	13.247	14.814	14.328	13.326	14.834
2457192.3160	P	EAST	13.203	12.466	12.252	12.462	12.242	12.845	12.796	12.745	12.285	12.693	13.811	13.125	14.411	13.048	13.248	14.864	14.353	13.325	14.808
2457192.3180	P	EAST	13.215	12.330	12.254	12.460	12.251	12.853	12.796	12.738	12.273	12.696	13.810	13.120	14.448	13.053	13.252	14.836	14.341	13.329	14.843
2457192.3210	P	EAST	13.194	12.267	12.236	12.463	12.242	12.840	12.787	12.730	12.278	12.691	13.862	13.118	14.415	13.077	13.248	14.860	14.310	13.335	14.791
2457192.3230	P	EAST	13.156	12.564	12.247	12.456	12.246	12.845	12.795	12.734	12.294	12.706	13.790	13.116	14.405	13.046	13.245	14.862	14.312	13.324	14.795
2457192.3250	P	EAST	13.388	12.436	12.255	12.465	12.242	12.858	12.793	12.740	12.291	12.693	13.790	13.118	14.436	13.040	13.246	14.830	14.327	13.318	14.831
2457192.3280	P	EAST	12.978	12.421	12.235	12.456	12.257	12.835	12.785	12.741	12.290	12.700	13.823	13.112	14.411	13.044	13.238	14.844	14.332	13.323	14.831
2457192.3300	P	EAST	12.414	12.471	12.238	12.455	12.259	12.844	12.779	12.741	12.289	12.698	13.806	13.107	14.409	13.045	13.243	14.841	14.330	13.321	14.809
2457192.2970	P	WEST	13.834	12.762	12.255	12.415	12.247	12.921	12.757	12.679	12.315	12.741	13.798	13.074	14.720	13.083	13.251	15.192	14.569	13.322	14.781
2457192.3020	P	WEST	14.270	12.755	12.248	12.420	12.230	12.908	12.763	12.688	12.335	12.711	13.800	13.095	14.708	13.065	13.269	15.186	14.551	13.336	14.801
2457192.3040	P	WEST	14.318	12.745	12.228	12.414	12.243	12.913	12.767	12.688	12.324	12.735	13.809	13.084	14.708	13.052	13.264	15.194	14.577	13.318	14.811
2457192.3060	P	WEST	14.338	12.739	12.220	12.406	12.242	12.918	12.782	12.707	12.319	12.705	13.812	13.108	14.694	13.060	13.259	15.161	14.583	13.300	14.790
2457192.3090	P	WEST	14.188	12.767	12.236	12.460	12.236	12.917	12.760	12.679	12.308	12.710	13.771	13.095	14.695	13.057	13.240	15.128	14.541	13.329	14.789
2457192.3110	P	WEST	14.116	12.766	12.230	12.449	12.233	12.923	12.775	12.680	12.307	12.712	13.801	13.080	14.678	13.072	13.260	15.120	14.522	13.323	14.761
2457192.3130	P	WEST	13.550	12.771	12.240	12.453	12.231	12.909	12.753	12.700	12.327	12.714	13.786	13.075	14.702	13.047	13.234	15.137	14.502	13.330	14.812
2457192.3160	P	WEST	13.421	12.765	12.244	12.454	12.231	12.899	12.789	12.701	12.307	12.704	13.816	13.086	14.659	13.059	13.268	15.119	14.489	13.340	14.769
2457192.3180	P	WEST	13.441	12.767	12.233	12.454	12.247	12.897	12.759	12.703	12.296	12.707	13.783	13.074	14.640	13.072	13.258	15.087	14.474	13.344	14.766
2457192.3210	P	WEST	13.451	12.762	12.252	12.417	12.240	12.909	12.796	12.693	12.312	12.731	13.806	13.100	14.697	13.048	13.249	15.066	14.453	13.344	14.798
2457192.3230	P	WEST	13.360	12.769	12.230	12.432	12.244	12.886	12.778	12.703	12.312	12.726	13.794	13.090	14.613	13.054	13.234	15.077	14.447	13.330	14.793
2457192.3250	P	WEST	13.586	12.766	12.238	12.439	12.243	12.868	12.772	12.712	12.317	12.727	13.785	13.077	14.627	13.051	13.264	15.073	14.468	13.336	14.794
2457192.3280	P	WEST	13.156	12.766	12.223	12.450	12.219	12.882	12.800	12.710	12.309	12.724	13.799	13.106	14.624	13.041	13.269	15.047	14.459	13.316	14.808
2457192.3300	P	WEST	12.613	12.770	12.236	12.435	12.240	12.859	12.770	12.718	12.317	12.735	13.792	13.080	14.580	13.047	13.258	15.067	14.471	13.330	14.813

Table 3. Photometry of V404 Cyg by MASTER-Kislovodsk Telescope in JD2457192.13-JD2457192.28

Table 4. ($I_{West} - I_{East}$)/($I_{West} + I_{East}$) of V404 Cyg by MASTER-Kislovodsk Telescope in JD2457192.13-JD2457192.28

JD	#1	#2	#3	#4	#5	#6	#7	#8	#9	#10	#11	#12	#13	#14	#15	#16	#17	#18	#19
2457192.2970	0.14225	0.03682	0.00000	-0.02072	0.00368	0.02992	-0.01842	-0.02302	0.00092	0.01796	0.01197	-0.01428	0.13638	0.02026	-0.00184	0.13819	0.10871	-0.00322	-0.00184
2457192.3020	0.15081	0.04280	-0.00553	-0.01980	-0.00230	0.01934	-0.01842	-0.01658	0.01335	0.00691	0.00553	-0.00691	0.13095	0.01243	0.00414	0.16204	0.10780	0.00461	0.00368
2457192.3040	0.13909	0.04924	-0.01566	-0.02210	0.00184	0.02302	-0.01980	-0.01381	0.00737	0.01704	0.01151	-0.01105	0.12280	0.00737	0.00737	0.15261	0.11962	-0.00461	0.01105
2457192.3060	0.12552	0.05199	-0.01289	-0.02486	0.00184	0.02946	-0.00829	-0.01105	0.01013	0.00184	0.01151	-0.00276	0.10780	0.00875	0.00230	0.14225	0.12370	-0.01612	-0.00921
2457192.3090	0.12370	0.07080	-0.00829	-0.00276	-0.00230	0.02256	-0.01612	-0.02072	0.00230	0.00737	-0.01013	-0.00599	0.11917	0.01151	-0.00461	0.12869	0.09732	0.00000	-0.01842
2457192.3110	0.11599	0.13231	-0.01289	-0.00276	-0.00276	0.02946	-0.01151	-0.02302	0.00322	0.00414	-0.00092	-0.01335	0.10598	0.01428	0.00276	0.11826	0.08865	-0.00368	-0.02072
2457192.3130	0.11371	0.10689	-0.00921	-0.00599	-0.00599	0.02578	-0.01658	-0.01381	0.01612	0.00599	-0.00368	-0.01980	0.11462	0.00046	-0.00599	0.14766	0.07996	0.00184	-0.01013
2457192.3160	0.10006	0.13683	-0.00368	-0.00368	-0.00507	0.02486	-0.00322	-0.02026	0.01013	0.00507	0.00230	-0.01796	0.11371	0.00507	0.00921	0.11689	0.06255	0.00691	-0.01796
2457192.3180	0.10370	0.19857	-0.00967	-0.00276	-0.00184	0.02026	-0.01704	-0.01612	0.01059	0.00507	-0.01243	-0.02118	0.08819	0.00875	0.00276	0.11508	0.06117	0.00691	-0.03544
2457192.3210	0.11780	0.22409	0.00737	-0.02118	-0.00092	0.03176	0.00414	-0.01704	0.01566	0.01842	-0.02578	-0.00829	0.12914	-0.01335	0.00046	0.09458	0.06576	0.00414	0.00322
2457192.3230	0.09367	0.09413	-0.00783	-0.01105	-0.00092	0.01888	-0.00783	-0.01428	0.00829	0.00921	0.00184	-0.01197	0.09550	0.00368	-0.00507	0.09869	0.06209	0.00276	-0.00092
2457192.3250	0.09093	0.15081	-0.00783	-0.01197	0.00046	0.00461	-0.00967	-0.01289	0.01197	0.01566	-0.00230	-0.01888	0.08773	0.00507	0.00829	0.11144	0.06484	0.00829	-0.01704
2457192.3280	0.08179	0.15755	-0.00553	-0.00276	-0.01750	0.02164	0.00691	-0.01428	0.00875	0.01105	-0.01105	-0.00276	0.09778	-0.00138	0.01428	0.09321	0.05842	-0.00322	-0.01059
2457192.3300	0.09139	0.13683	-0.00092	-0.00921	-0.00875	0.00691	-0.00414	-0.01059	0.01289	0.01704	-0.00645	-0.01243	0.07859	0.00092	0.00691	0.10370	0.06484	0.00414	0.00184